Received: 19 March 2021 | Revised: 9 July 2021 | Accepted: 19 July 2021

DOI: 10.1002/jcp.30539

RESEARCH ARTICLE

Journal of Cellular Physiology WILEY

PGC-1α regulates myonuclear accretion after moderate endurance training

Edmund Battey[1,2] | Regula Furrer[3] | Jacob Ross[2] | Christoph Handschin[3] | Julien Ochala[1,4,5] | Matthew J. Stroud[2]

[1]Centre of Human and Applied Physiological Sciences, School of Basic and Medical Biosciences, Faculty of Life Sciences & Medicine, King's College London, London, UK

[2]British Heart Foundation Centre of Research Excellence, School of Cardiovascular Medicine and Sciences, Faculty of Life Sciences & Medicine, King's College London, London, UK

[3]Biozentrum, University of Basel, Basel, Switzerland

[4]Randall Centre for Cell and Molecular Biophysics, School of Basic & Medical Biosciences, Faculty of Life Sciences & Medicine, Guy's Campus, King's College London, London, UK

[5]Department of Biomedical Sciences, University of Copenhagen, Copenhagen, Denmark

Correspondence

Matthew J. Stroud, British Heart Foundation Centre of Research Excellence, School of Cardiovascular Medicine and Sciences, Faculty of Life Sciences & Medicine, King's College London, London, SE5 9NU, UK.
Email: matthew.stroud@kcl.ac.uk

Funding information

British Heart Foundation, Grant/Award Numbers: FS/17/57/32934, RE/18/2/34213; Medical Research Council, Grant/Award Number: MR/S023593/1

Abstract

The transcriptional demands of skeletal muscle fibres are high and require hundreds of nuclei (myonuclei) to produce specialised contractile machinery and multiple mitochondria along their length. Each myonucleus spatially regulates gene expression in a finite volume of cytoplasm, termed the myonuclear domain (MND), which positively correlates with fibre cross-sectional area (CSA). Endurance training triggers adaptive responses in skeletal muscle, including myonuclear accretion, decreased MND sizes and increased expression of the transcription co-activator peroxisome proliferator-activated receptor-γ coactivator-1α (PGC-1α). Previous work has shown that overexpression of PGC-1α in skeletal muscle regulates mitochondrial biogenesis, myonuclear accretion and MND volume. However, whether PGC-1α is critical for these processes in adaptation to endurance training remained unclear. To test this, we evaluated myonuclear distribution and organisation in endurance-trained wild-type mice and mice lacking PGC-1α in skeletal muscle (PGC-1α mKO). Here, we show a differential myonuclear accretion response to endurance training that is governed by PGC-1α and is dependent on muscle fibre size. The positive relationship of MND size and muscle fibre CSA trended towards a stronger correlation in PGC-1a mKO versus control after endurance training, suggesting that myonuclear accretion was slightly affected with increasing fibre CSA in PGC-1α mKO. However, in larger fibres, the relationship between MND and CSA was significantly altered in trained versus sedentary PGC-1α mKO, suggesting that PGC-1α is critical for myonuclear accretion in these fibres. Accordingly, there was a negative correlation between the nuclear number and CSA, suggesting that in larger fibres myonuclear numbers fail to scale with CSA. Our findings suggest that PGC-1α is an important contributor to myonuclear accretion following moderate-intensity endurance training. This may contribute to the adaptive response to endurance training by enabling a sufficient rate of transcription of genes required for mitochondrial biogenesis.

KEYWORDS

endurance exercise, mitochondria, myonuclei, PGC-1 α, skeletal muscle

1 | INTRODUCTION

Skeletal muscle fibres contain specialised contractile machinery and thousands of mitochondria along their length (from several millimetres to centimetres) (Frontera & Ochala, 2015; Lieber, 2002). The transcriptional demands of these large, protein-rich cells are high and require hundreds of nuclei, termed myonuclei. Myonuclei regulate gene products in local volumes of cytoplasm, termed myonuclear domains (MNDs) (Allen et al., 1999; Hall & Ralston, 1989; Pavlath et al., 1989). In normal muscle, MND volume correlates with fibre cross-sectional area (CSA), with larger fibres having larger MNDs than small fibres (Bruusgaard et al., 2003).

MND size is inversely correlated with mitochondrial number as demonstrated by a study in which peroxisome proliferator-activated receptor (PPAR)-γ coactivator-1α (PGC-1α), a regulator of mitochondrial biogenesis, was specifically up- and downregulated in skeletal muscle (Ross et al., 2017). PGC-1α is a transcriptional coactivator and binds to a variety of transcription factors, including mitochondrial transcription factor A, oestrogen-related receptor alpha, PPAR-α and nuclear respiratory factors (Scarpulla, 2011; Schreiber et al., 2003; Uldry et al., 2006; Wu et al., 1999). This, in turn, enhances the expression of mitochondrial genes and genes involved in oxidative phosphorylation (such as ATP synthase, cytochrome *c* and cytochrome *c* oxidase subunits II and IV) and fatty acid oxidation, thereby promoting mitochondrial biogenesis and oxidative metabolism (Scarpulla, 2011; Schreiber et al., 2004; Uldry et al., 2006; Wu et al., 1999). When overexpressed in a muscle-specific manner, PGC-1α leads to myonuclear accretion and decreases MND volume, which is hypothesised to allow sufficient transcription and synthesis of energy-demanding mitochondria-related proteins (Ross et al., 2017).

Myonuclear accretion and decreased MND size can also occur in endurance-trained (ET) skeletal muscle (Goh et al., 2019), in which PGC-1α expression and mitochondrial biogenesis are also enhanced (Baar et al., 2002; Goh et al., 2019; Irrcher et al., 2003; Pilegaard et al., 2003). Specifically, in response to such functional and metabolic demands, satellite cell number and activation are increased, new myonuclei are generated and ultimately MND sizes are decreased (Abreu et al., 2017; Allen et al., 1999; Cisterna et al., 2016; Smith & Merry, 2012). From these findings, it is tempting to hypothesise that greater PGC-1α content caused by endurance training may regulate MND volume.

In addition to its potential role in myonuclear accretion, PGC-1α may affect nuclear shape (Ross et al., 2017), which can also affect gene expression (Battey et al., 2020; Dahl et al., 2008; Lammerding et al., 2005). Specifically, our previous work showed that overexpression of PGC-1α in the diaphragm increases the roundness of myonuclei, and removal of PGC-1α results in elongated myonuclei in extensor digitorum longus (EDL) muscle fibres (Ross et al., 2017). However, whether these effects are observed in other muscle fibres remained to be established.

In the present study, we aimed to test whether PGC-1α is necessary for remodelling myonuclear number, MND sizes and nuclear morphology after endurance training. To this end, we investigated the effects of moderate-intensity endurance training on myonuclear distribution, organisation and shape in tibialis anterior (TA) muscle of wild-type (WT) mice and mice lacking PGC-1α in skeletal muscle (PGC-1α mKO) (Levy et al., 2018; Ross et al., 2017). We found PGC-1α governs scaling of both MND and myonuclear number with fibre CSA in larger muscle fibres of ET mice, suggesting that PGC-1α regulates myonuclear accretion in larger muscle fibres following endurance training.

2 | METHODS

2.1 | Mouse genotypes and endurance training protocol

Mice were housed with free access to food and water in a conventional facility with a 12-h night and day cycle and all experiments were approved by Kantonales Veterinäramt Basel-Stadt, Switzerland. PGC-1α muscle-specific knockout (mKO) mice were generated by crossing *PGC-1α*$^{loxP/loxP}$ mice with human α-skeletal actin promoter (HSA)-Cre transgenic mice, as described previously (Lin et al., 2002; Miniou et al., 1999; Pérez-Schindler et al., 2013). To investigate whether PGC-1α is required for remodelling myonuclear number and MND sizes in response to endurance exercise, 20-week-old WT and PGC-1α mKO mice were split into one group to be endurance-trained and one group to be left sedentary. The 4-week progressive endurance training programme consisted of 1 h of treadmill running per day, five times per week. The treadmill slope was set to 5° and the starting velocity was 10 m/min and was increased by 0.5 m/min every day. TA muscle was harvested from mice that were sacrificed 72 h after the endurance training programme to exclude potential confounding effects observed acutely after exercise (Carmichael et al., 2005; Neubauer et al., 2014). Thus, the groups were as follows: WT ($n = 5$), WT ET ($n = 5$), PGC-1α mKO ($n = 5$), PGC-1α mKO ET ($n = 5$).

2.2 | Preparation, staining and imaging isolated fibres

2.2.1 | Preparation

TA muscle samples were snap-frozen in liquid nitrogen and processed for storage and experiments as follows. Samples were placed in a relaxing solution (1 mM $MgCl_2$, 5 mM ATP, 100 mM KCl, 10 mM imidazole, 2 mM EGTA [pH 7], 100 mM KCl) on ice, divided into bundles of ~50–100 myofibres, and then chemically skinned in skinning solution (relaxing solution containing glycerol, 1:1 v/v), at 4°C for 24 h. Fibres were then stored at −20°C in a skinning solution for up to 4 weeks.

For analyses of myonuclear arrangement and shape through confocal microscopy imaging, fibres were mounted as described by

Levy et al. (2018): the ends of fibres were clamped using the free ends of half-split copper transmission electron microscopy (TEM) meshes (SPI G100 2010C-XA, width 3 mm) glued to glass coverslips (Menzel-Gläser, 22 × 50 mm, thickness 0.13–0.16 mm) at comparable tensions (~2.4 μm) to allow standardised comparisons of myonuclear shape and arrangement.

2.2.2 | Staining

4′,6-Diamidino-2-phenylindole (DAPI) (Molecular Probes, D3571; Thermo Fisher Scientific) and Rhodamine Phalloidin (Biotum) were diluted 1:1000 and 1:100 in phosphate-buffered saline (PBS) to visualise myonuclei and filamentous actin, respectively.

To analyse myonuclear morphology and visualise nuclear envelope proteins, PFA-fixed fibres were immunostained as follows. Fibres were permeabilised with 0.1% Triton X-100 in PBS for 10 min then stained with DAPI and Rhodamine Phalloidin for 1.5 h at room temperature. After washing thrice in PBS, fibres were mounted in Fluoromount-G® (Southern Biotech) on TEM meshes between two glass coverslips for assessment of myonuclear arrangement and morphology.

2.2.3 | Imaging

A Zeiss Axiovert 200 microscope with a Photometrics CoolSNAP HQ camera was used in conjunction with Metamorph software to acquire images for myonuclear arrangement and 2D morphological analyses. For myonuclear arrangement analyses, Z-stacks of 100 images, in 1-μm increments, were acquired using a ×20 air objective. For analysis of nuclear morphology, single images were acquired using a ×40 air objective.

2.3 | Image analysis

2.3.1 | Nuclear arrangement

Analysis of nuclear arrangement was carried using Metamorph software. Z-stacks were imported, and each nucleus within the field of view (using DAPI signal), edges of fibres in the *XY* and *Z* planes (using phalloidin signal) were recorded on Excel (linked to Metamorph) and these data were analysed using a MATLAB script to obtain MND (volume of cytoplasm governed by each nucleus), order score (spatial distribution of nuclei), nearest neighbour distance (distance between nuclei) and fibre dimension values (Bruusgaard et al., 2003). For nuclear arrangement analyses, fibres were categorised into smaller and larger groups using the median CSA values from each group to ensure standardised comparisons of muscle fibre size between the groups. An average of 6.9 ± 1.1 fibres (mean ± SD) was analysed per group. The number of fibres analysed for each group (mean, range) were WT (5.8, 5–7); WT ET (6.4, 4–7); PGC-1α mKO (7.8, 7–9); PGC-1α ET (8, 5–10); $N = 5$ mice per group.

2.3.2 | Characterisation of nuclear area and shape

To quantify 2D nuclear shape parameters (nuclear area and aspect ratio), images were analysed using Fiji software as described previously (Stroud et al., 2017). Images were processed with a rolling ball background subtraction (150 pixels), Gaussian blur filter (2 pixels radius) and despeckle function before thresholding the DAPI signal (initially with 'Otsu dark' setting then adjusting as necessary) and recording particle analysis results, manually checking the images for any incorrectly thresholded or overlapping nuclei. Laterally located nuclei (longitudinal plane) were excluded from analysis as nuclei in this position are orientated perpendicular, rather than parallel, to the objective lens. In total, 9–18 fibres and 169–254 nuclei were analysed per mouse ($N = 5$ mice per group).

2.3.3 | Fibre typing

To determine fibre type proportions, 10-μm-thick cryosections of TA muscle were cut in transverse orientation, air-dried on slides and stored at −80°C as described previously (Stroud et al., 2018). Before staining, slides were thawed, dried for 10 min and rehydrated in PBS for 10 min. Sections were then blocked in 1% bovine serum albumin/PBS for 10 min. Antibodies directed against myosin isoforms were then applied in blocking buffer overnight at room temperature at dilutions of 1:30: mouse anti-myosin slow/type I (IgG2b isoform, clone BA-F8); mouse anti-myosin fast/type IIA (IgG1 isoform, clone SC-71); mouse anti-myosin fast/type IIX (IgM isoform, clone 6H1); mouse anti-myosin fast/type IIb (IgM isoform, clone BF-F3). Sections were then washed in PBS/0.025% Tween-20, and incubated with isotype-specific secondary antibodies conjugated to Alexa 488 or 555 in blocking buffer (dilution 1:500) for 5 h. Finally, slides were washed in PBS, mounted in Dako mounting medium. Sections were imaged using a ×10 air objective and the proportion of each fibre type was quantified by dividing the total number of fibres in the field of view by the number of fibres with positive staining for each antibody. BA-F8 antibody revealed there were no type I fibres in the sections so fibres that did not bind with SC-71 and 6H1 antibodies were determined to be type IIB fibres.

2.4 | Statistical analysis

Statistical analyses were performed using GraphPad Prism software (GraphPad, version 8). For correlation analyses, a simple linear regression was performed to test if slopes were significantly non-zero and nonlinear straight-line regression

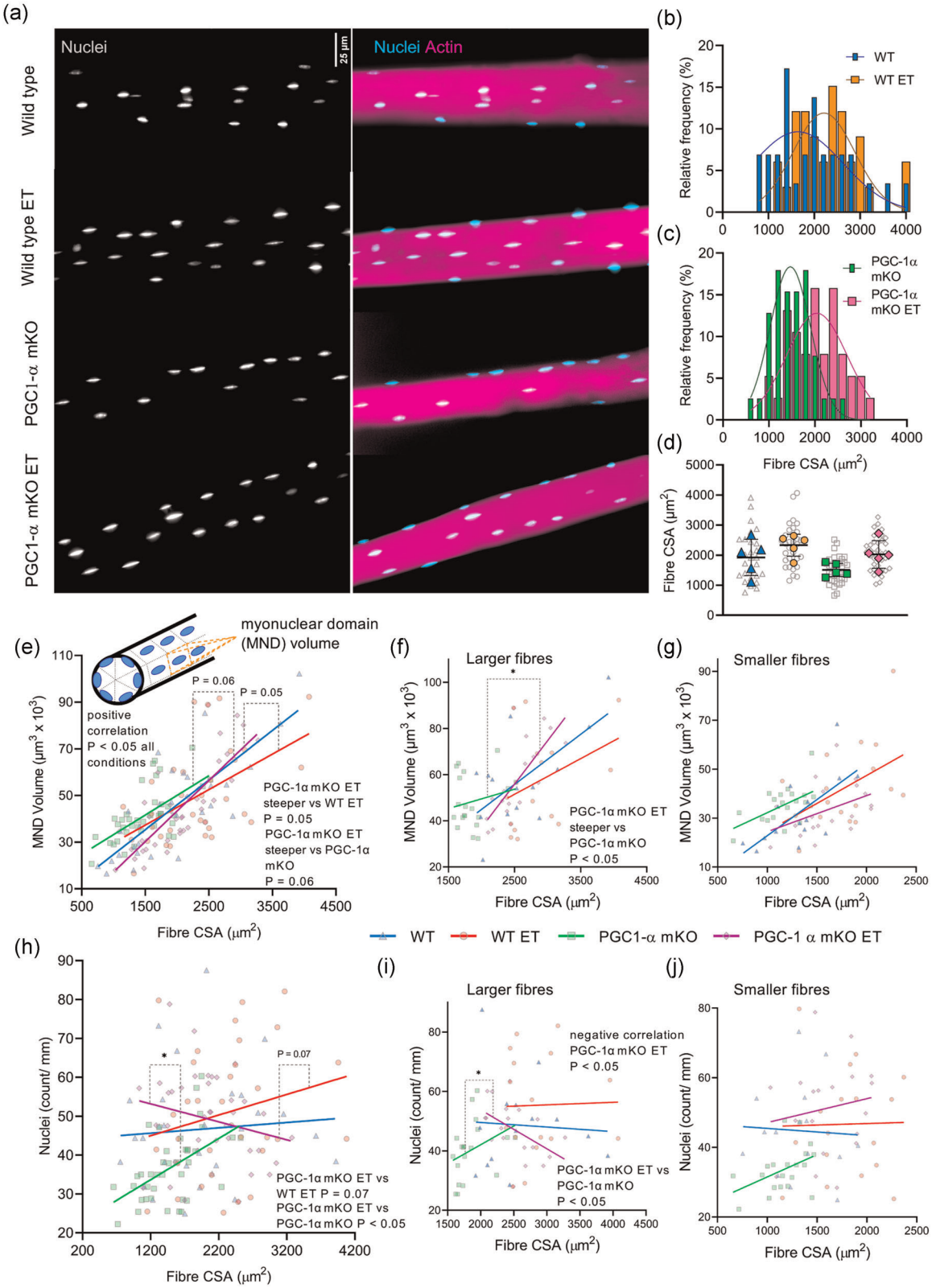

FIGURE 1 (See caption on next page)

analyses were performed to compare the slopes of a different condition. To analyse whether an overall significant difference was present between muscle fibres from the different groups (myonuclear area, myonuclear aspect ratio, order score), two-way analysis of variance (ANOVA) was carried out, followed by post-hoc Tukey tests to specify between which groups differences existed. Mean values for each mouse were used for two-way ANOVA tests ($n = 5$). $p < 0.05$ indicated significance and $p < 0.07$ indicated a trend for regression and ANOVA analyses.

3 | RESULTS

3.1 | PGC-1α differentially regulates MND:CSA scaling after endurance training in larger muscle fibres

Previously, endurance training and overexpression of the peroxisome proliferator-activated receptor-γ coactivator-1α (PGC-1α) have been shown to favour myonuclear accretion, thus decreasing MND size (Allen et al., 1999; Baar et al., 2002; Cisterna et al., 2016; Irrcher et al., 2003; Pilegaard et al., 2003; Ross et al., 2017; Smith & Merry, 2012). To test whether the myonuclear accretion and decreased MND size following endurance exercise is dependent on PGC-1α, we compared fibre CSA, myonuclear number and domain size in trained and sedentary WT and PGC-1α mKO mice. There were no significant differences in fibre CSA or fibre type proportions between WT and PGC-1α mKO mice, with or without endurance training (Figures 1a–d and S1).

We next focused on the relationship between MND and CSA, which has been shown to positively correlate in normal muscle fibres (Bruusgaard et al., 2003), with larger fibres possessing larger MNDs than smaller fibres. In line with this, we observed this relationship when looking at all fibre sizes grouped together (Figure 1e and Table 1). However, we noticed a trend towards a steeper relationship between PGC-1α mKO versus control after training ($p = 0.05$) and between sedentary and exercised PGC-1α mKO ($p = 0.06$), suggesting that PGC-1α may play a subtle role in regulating myonuclear accretion (Figure 1e and Table 1). In contrast to the smaller fibres, we noticed that in larger fibres the correlation between MND and fibre CSA was significantly steeper in PGC-1α mKO exercised compared with PGC-1α mKO sedentary mice, suggesting that PGC-1α may differentially regulate myonuclear accretion in these larger fibres ($p < 0.05$; Figure 1f,g and Table 1). In support of these findings, there was a negative correlation between the nuclear number and fibre CSA in larger PGC-1α mKO ET fibres ($p < 0.05$; Figure 1h–i and Table 1). This indicates that in the absence of PGC-1α, the addition of new myonuclei in response to endurance training does not follow the known MND–fibre size relationship (Bruusgaard et al., 2003).

In addition to the nuclear number, MND is governed by the spatial organisation of myonuclei. To assess this, we quantified order scores (*g*), which indicate how ordered the distribution of myonuclei are (Bruusgaard et al., 2003). Fibres with evenly spaced nuclei have higher-order scores, and those with uneven spacing have lower-order scores. We did not find any significant differences in order scores between the various groups, suggesting proper internuclear spacing in the absence of PGC-1α (Figure 2a–c). Importantly, these data suggest that the altered relationship between MND and CSA observed in larger fibres is due to altered myonuclear accretion rather than altered spatial distribution of myonuclei.

Overall, our data indicate that PGC-1α is required for MND remodelling following endurance training and thereby allows the maintenance of the nuclear number-fibre size paradigm (Bruusgaard et al., 2003).

3.2 | PGC-1α does not regulate nuclear shape in response to endurance training in TA muscle fibres

Since overexpression of PGC-1α has previously been shown to increase the roundness of myonuclei, and lack of PGC-1α can result in elongated myonuclei (Ross et al., 2017), we investigated whether PGC-1α regulates nuclear morphology in response to moderate endurance training. To characterise nuclear morphology, we quantified myonuclear area and myonuclear aspect ratio (a measure of myonuclear elongation). Myonuclear area was 20%

FIGURE 1 PGC-1α is required for the myonuclear number to scale with muscle fibre cross-sectional area (CSA) after moderate endurance training. (a) Representative images of isolated muscle fibres stained with 4′,6-diamidino-2-phenylindole (DAPI) to visualise myonuclei (blue), and phalloidin to visualise actin filaments (magenta), in wild type (WT), wild-type endurance-trained (WT ET), PGC-1α muscle-specific knockout (PGC-1α mKO) and PGC-1α muscle-specific knockout endurance-trained (PGC-1α mKO ET) mice. (b, c) Relative frequency (%) of muscle fibre cross-sectional area (CSA; μm^2) in 200 μm^2 intervals. (d) Comparison of muscle fibre CSA; two-way analysis of variance comparisons of mean fibre CSA for each mouse ($n = 5$ per group) indicated no genotype or training effect; coloured symbols represent averaged values for each mouse, unfilled grey symbols represent individual muscle fibres, error bars indicate mean ± SD. (e–f) Myonuclear domain (MND) volume was plotted against fibre CSA in all fibres (e), larger fibres (f) and smaller fibres (g). Note the trend towards a stronger correlation between PGC-1a mKO ET with both WT ET and PGC1a mKO and that in larger fibres (>median) the MND-CSA correlation was significantly steeper in PGC-1α mKO ET compared with PGC-1α mKO. (h–j) Number of nuclei plotted against fibre CSA in all fibres (h), larger fibres (i) and smaller fibres (j). Note the negative correlation between the nuclear number and fibre CSA in PGC-1a mKO ET in larger fibres. (e–j) Coloured symbols represent individual muscle fibres. In total, 5–10 fibres were analysed per mouse; $n = 5$ mice per group. Simple linear regression and straight-line nonlinear regression were performed for correlation analyses. $^*p < 0.05$. See Table 1 for R^2 and p values

TABLE 1 Myonuclear domain (MND) ($\mu m^3 \times 10^3$) and nuclei (count/mm) correlated with fibre cross-sectional area (CSA): R^2 and p values

	WT			WT ET			PGC-1α mKO			PGC-1α mKO ET		
	All fibres	Smaller fibres	Larger fibres	All fibres	Smaller fibres	Larger fibres	All fibres	Smaller fibres	Larger fibres	All fibres	Smaller fibres	Larger fibres
MND ($\mu m^3 \times 10^3$) versus CSA (μm^2)												
R^2	0.64	0.46	0.42	0.28	0.23	0.14	0.38	0.32	0.04	0.64	0.18	0.55
p												
Correlation	<0.01*	<0.01*	0.01*	<0.01*	0.05**	0.15	<0.01*	0.01*	0.42	<0.01*	0.07**	<0.01*
Versus WT ET	0.27	0.65	0.62	-			-			-		
Versus PGC-1α mKO	0.38	0.35	0.33	0.79	0.78	0.67	-			-		
Versus PGC-1α mKO ET	0.28	0.21	0.19	0.05**	0.36	0.13	0.06**	0.15	0.04*	-		
Nuclei (count/mm) versus CSA (μm^2)												
R^2	0.01	<0.01	<0.01	0.05	<0.01	<0.01	0.26	0.19	0.12	0.05	0.02	0.24
p												
Correlation	0.69	0.86	0.84	0.22	0.94	0.93	0.01*	0.05**	0.15	0.18	0.52	0.04*
Versus WT ET	0.47	0.86	0.84	-			-			-		
Versus PGC-1α mKO	0.07**	0.27	0.27	0.36	0.41	0.41	-			-		
Versus PGC-1α mKO ET	0.22	0.57	0.26	0.07**	0.70	0.23	<0.01*	0.66	0.01*	-		

Note: Muscle fibres from age-matched WT, WT ET, PGC-1α mKO (PGC-1α muscle-specific knockout) and PGC-1α mKO ET (PGC-1α muscle-specific knockout endurance-trained) mice were analysed. 'Correlation' p values indicate whether the relationship is significant, versus p values show whether the differences between slopes from different conditions were significant. Straight-line nonlinear regression analyses. See Figure 1 for correlation graphs.

Abbreviations: CSA, cross-sectional area; mKO, muscle-specific knockout; MND, myonuclear domain; WT, wild type; WT ET, wild-type endurance-trained.

*Statistical significance ($p < 0.05$).

**Trends ($p < 0.07$).

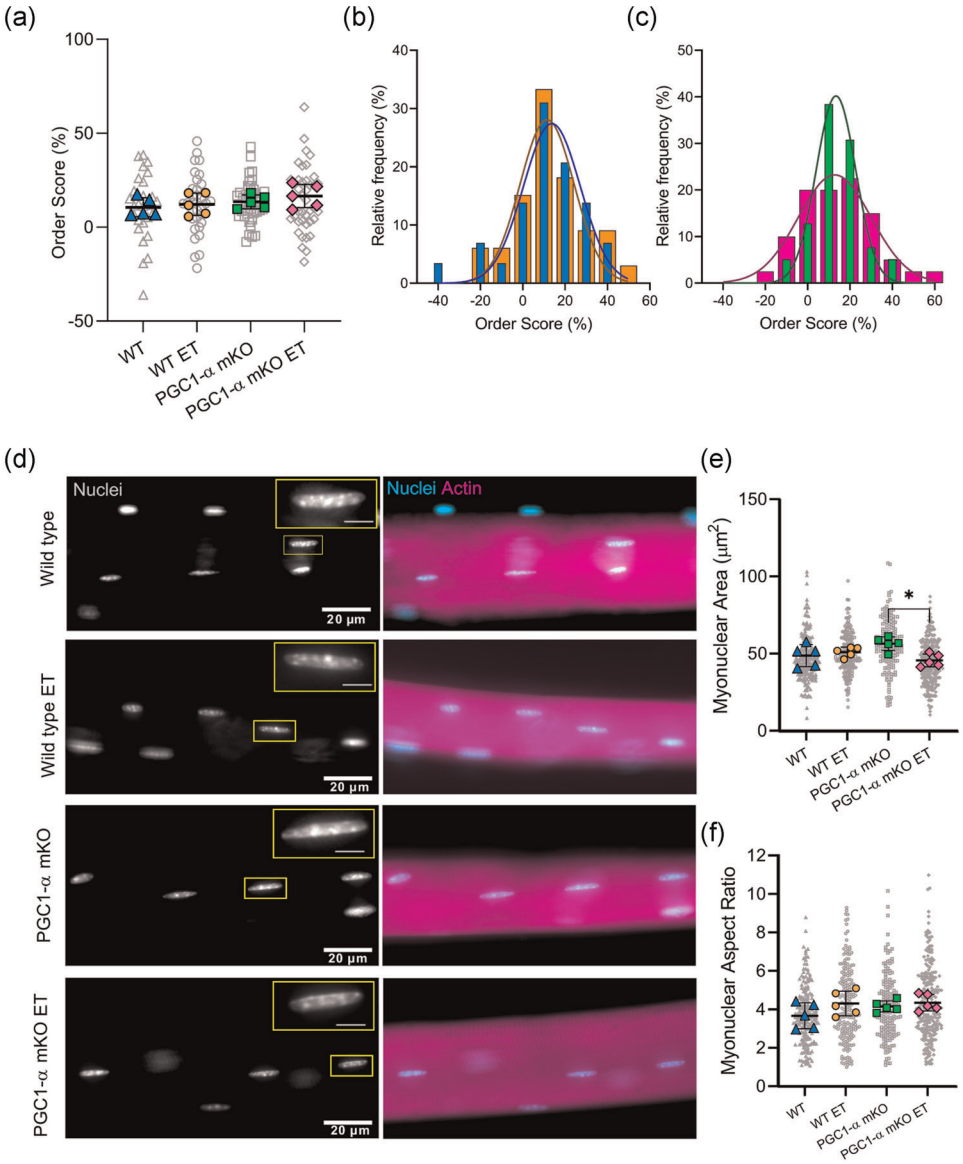

FIGURE 2 Myonuclear arrangement was comparable across groups; endurance-trained mice lacking PGC-1α have reduced myonuclear area compared with sedentary mice lacking PGC-1α. (a) Comparisons of mean order score (%) in wild type (WT), wild type endurance-trained (WT ET), PGC-1α muscle-specific knockout (PGC-1α mKO) and PGC-1α mKO endurance-trained (PGC-1α mKO ET) mice. No significant differences were observed between groups (two-way analysis of variance [ANOVA] using mean values for each mouse; $n = 5$). (b,c) Relative frequency (%) of order score (%) in 10% intervals. (a–c) In total, 5–10 fibres were analysed per mouse; $n = 5$ mice per group. (d) Representative images of muscle fibres isolated from WT, WT ET, PGC-1α mKO and PGC-1α mKO ET stained with 4′,6-diamidino-2-phenylindole (DAPI) (cyan) and phalloidin (magenta) to visualise myonuclei and actin filaments, respectively. Scale bars in zoomed insets of myonuclei, 10 µm. (e) Comparisons of the myonuclear area in WT, WT ET, PGC-1α mKO and PGC-1α mKO ET mice. Note that myonuclear area was significantly reduced in PGC-1α mKO ET mice compared with PGC-1α mKO mice (*$p < 0.05$, two-way ANOVA). (f) Comparisons of myonuclear aspect ratio in WT, WT ET, PGC-1α mKO and PGC-1α mKO ET. No significant differences were observed between groups (two-way ANOVA). (e,f) $n = 5$ mice per group, 169–254 nuclei analysed per mouse, 815 nuclei analysed total, mean values for each mouse used for two-way ANOVA tests ($n = 5$). Coloured symbols represent individual mice, unfilled grey symbols represent individual myonuclei

lower in endurance-trained PGC-1α mKO mice compared with sedentary PGC-1α mKO mice, but there were no significant differences when compared with WT mice (Figure 2d,e). The myonuclear aspect ratio was not significantly different between conditions (Figure 2f).

These results suggest that in contrast to diaphragm and EDL muscle fibres (Ross et al., 2017), PGC-1α does not influence myonuclear shape in TA muscle fibres. However, the myonuclear area is reduced after endurance training in mice lacking PGC-1α, an effect not observed in WT mice.

4 | DISCUSSION

We aimed to investigate whether transcriptional co-activator PGC-1α regulates myonuclear remodelling in endurance-trained muscle fibres. To achieve this, we studied a transgenic mouse model lacking expression of PGC-1α in skeletal muscle (Pérez-Schindler et al., 2013). Our results demonstrate that PGC-1α is an important regulator of myonuclear accretion following endurance training in larger fibres. The relationship between MND and fibre CSA was normal in smaller fibres from all groups, but in PGC-1α mKO mice, training resulted in relatively fewer myonuclei and therefore larger MNDs in larger fibres (Figure 3).

Endurance training promotes mitochondrial biogenesis in skeletal muscle fibres, driven by elevated PGC-1α expression (Baar et al., 2002; Goh et al., 2019; Irrcher et al., 2003; Pilegaard et al., 2003). Our findings suggest that PGC-1α may contribute to myonuclear accretion in muscle fibres in response to endurance training, helping to meet the increased demand to produce mitochondrial proteins.

An important mechanism of myonuclear addition is from the fusion of muscle stem cells, termed satellite cells, into the main muscle fibre (Petrella et al., 2008; Relaix & Zammit, 2012). Here, we generated PGC-1α muscle-specific knockout mice using a Cre mouse line under the control of human α-skeletal actin promoter (HSA-Cre). As HSA-Cre (Miniou et al., 1999) is not active in satellite cells, we interpret that the observed alterations to myonuclear addition originated intrinsically in muscle fibres and were caused by defective muscle fibre–satellite cell crosstalk. The HSA gene is switched on during myogenesis (Sassoon et al., 1988), so while the contribution of knocking out PGC-1α during this process might be small in this context, it cannot be completely ruled out. To address this, a conditional knockout model in which PGC-1α is only ablated in mature, differentiated myonuclei could be analysed. The mechanism by which PGC-1α may contribute to decreased MND volumes in larger muscle fibres after endurance training, and whether the trends observed are more striking after higher intensity training programmes, would be an interesting area for further research.

In the present study, we observed unchanged myonuclear number and MND volumes following endurance training in wild-type mice, suggesting that these parameters may only change in response to higher intensity training where hypertrophy is stimulated. It is well documented that myonuclear number increases in response to resistance training, which is associated with increased muscle fibre hypertrophy (Petrella et al., 2008). However, the effects of endurance training on MND volumes and myonuclear number change appear to depend on the intensity of training and whether hypertrophy occurs. Following 8 weeks of high-intensity endurance training in mice, the myonuclear

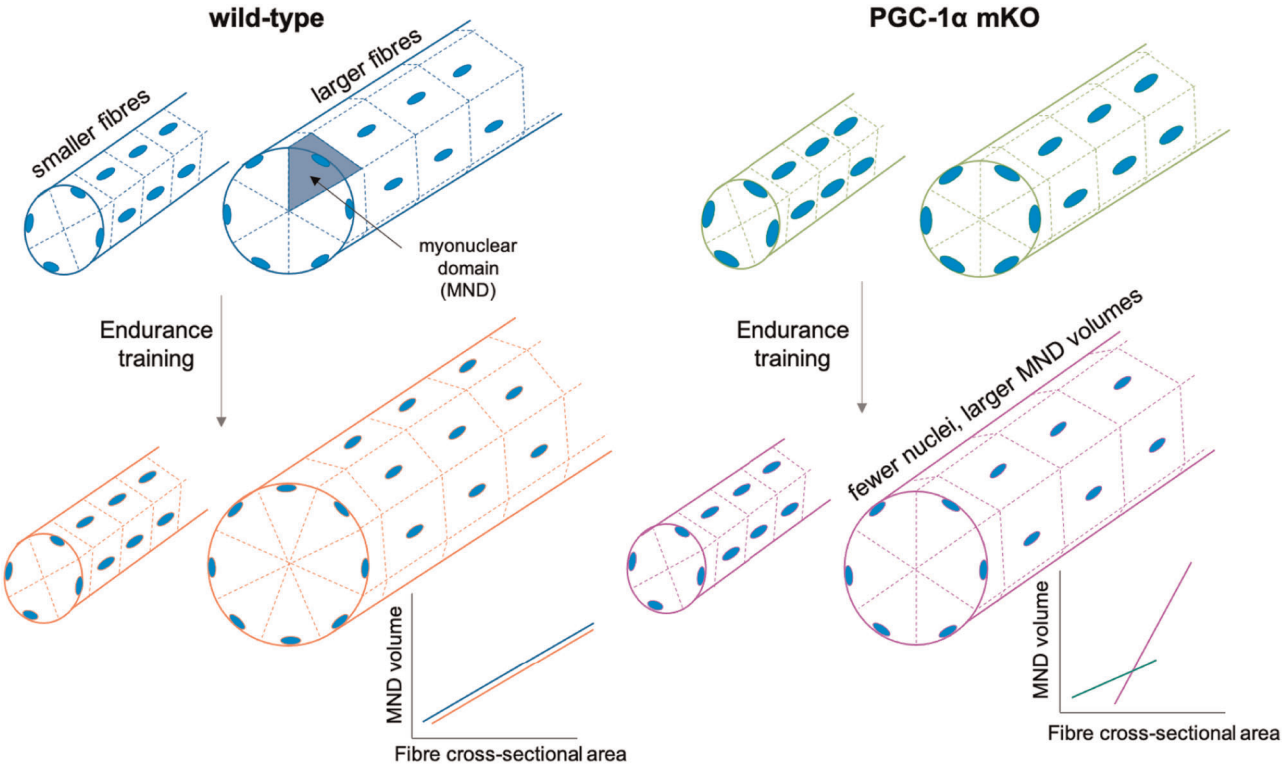

FIGURE 3 Working model showing the relationship between fibre size and myonuclear domain volumes in endurance-trained mice lacking PGC-1α. In mice lacking PGC-1α, moderate-intensity endurance training resulted in fewer myonuclei and thus larger myonuclear domain (MND) volumes in larger fibres compared with sedentary mice. This suggests PGC-1α is required for scaling of myonuclear number and MND volumes with fibre cross-sectional area (CSA). Dotted lines represent MND boundaries, blue ovals represent myonuclei

number was increased and associated with muscle fibre hypertrophy (Goh et al., 2019). Here, we found that moderate-intensity training did not result in hypertrophy or changes to the nuclear number or MND volumes, which is in line with Kurosaka and colleagues' findings in rat plantaris muscle following 10 weeks of low- or high-intensity endurance training (Kurosaka et al., 2012). Collectively, these findings suggest that myonuclear accretion and decreased MND volumes may occur to facilitate muscle hypertrophy but are not required for metabolic endurance training adaptations. Additionally, our findings in endurance-trained PGC-1α mKO mice suggest that PGC-1α may be required to maintain the myonuclear number and MND volumes in larger fibres after endurance training.

Altered nuclear morphology is associated with changes in how nuclei respond to forces, which are thought to be responsible for stimulating adaptations to exercise training (Coffey & Hawley, 2007; Earle et al., 2019). We investigated whether PGC-1α may be responsible for altering myonuclear shape following endurance training but observed no differences across study groups. This is in contrast to other hindlimb muscle groups, in which myonuclei were recently shown to be more circular following endurance training (Murach et al., 2020). Additionally, it is possible that a training intensity higher than ~60%–70% VO_2max would be required to produce enough force stimulation to elicit changes in myonuclear shape in the TA muscle. Despite consistent aspect ratios across groups, we observed smaller myonuclear areas in endurance-trained PGC-1α mKO mice compared with sedentary PGC-1α mKO mice. The biological significance of these data is unclear because the nuclear area in PGC-1α mKO mice was comparable to wild-type mice. Whether high-intensity endurance training influences myonuclear shape and size in TA muscle is a worthwhile area for further research.

A limitation of the comparisons of MND and number between conditions is that data were stratified into smaller and larger fibres based on relative rather than absolute size. Median fibre CSA for each condition was used to group data because a comparison of outcomes based on absolute fibre size was not possible due to different fibre size distributions in each group. Whilst we acknowledge this limitation, we are confident that the analyses completed provide pertinent insights into myonuclear parameters in fibres from PGC-1α mKO trained and untrained mice.

To conclude, we have demonstrated that PGC-1α is involved in controlling myonuclear accretion in larger muscle fibres in response to moderate-intensity endurance training. This may contribute to the adaptive response to endurance training by enabling a sufficient rate of transcription of genes required for mitochondrial biogenesis.

ACKNOWLEDGEMENTS

We thank the Medical Research Council (MR/S023593/1) and British Heart Foundation (FS/17/57/32934 and RE/18/2/34213) for support. Julien Ochala and Edmund Battey are funded by the Medical Research Council of the UK (MR/S023593/1). Matthew J. Stroud is supported by British Heart Foundation Intermediate Fellowship: FS/17/57/32934 and King's BHF Centre for Award Excellence: RE/18/2/34213.

CONFLICT OF INTERESTS

The authors declare that there are no conflict of interests.

ORCID

Julien Ochala http://orcid.org/0000-0002-6358-2920

Matthew J. Stroud http://orcid.org/0000-0002-3337-6851

REFERENCES

Abreu, P., Mendes, S. V. D., Ceccatto, V. M., & Hirabara, S. M. (2017). Satellite cell activation induced by aerobic muscle adaptation in response to endurance exercise in humans and rodents. *Life Sciences*, *170*, 33–40. https://doi.org/10.1016/j.lfs.2016.11.016

Allen, D. L., Roy, R. R., & Reggie Edgerton, V. (1999). Myonuclear domains in muscle adaptation and disease. *Muscle and Nerve*, *22*(10), 1350–1360. https://doi.org/10.1002/(SICI)1097-4598(199910)22:10%3C1350::AID-MUS3%3E3.0.CO;2-8

Baar, K., Wende, A. R., Jones, T. E., Marison, M., Nolte, L. A., Chen, M., Kelly, D. P., & Holloszy, J. O. (2002). Adaptations of skeletal muscle to exercise: Rapid increase in the transcriptional coactivator PGC-1. *The FASEB Journal*, *16*(14), 1879–1886. https://doi.org/10.1096/fj.02-0367com

Battey, E., Stroud, M. J., & Ochala, J. (2020). Using nuclear envelope mutations to explore age-related skeletal muscle weakness. *Clinical Science*, *134*(16), 2177–2187. https://doi.org/10.1042/CS20190066

Bruusgaard, J. C., Liestøl, K., Ekmark, M., Kollstad, K., & Gundersen, K. (2003). Number and spatial distribution of nuclei in the muscle fibres of normal mice studied in vivo. *Journal of Physiology*, *551*(2), 467–478. https://doi.org/10.1113/jphysiol.2003.045328

Carmichael, M. D., Davis, J. M., Murphy, E. A., Brown, A. S., Carson, J. A., Mayer, E., & Ghaffar, A. (2005). Recovery of running performance following muscle-damaging exercise: Relationship to brain IL-1β. *Brain, Behavior, and Immunity*, *19*(5), 445–452. https://doi.org/10.1016/j.bbi.2005.03.012

Cisterna, B., Giagnacovo, M., Costanzo, M., Fattoretti, P., Zancanaro, C., Pellicciari, C., & Malatesta, M. (2016). Adapted physical exercise enhances activation and differentiation potential of satellite cells in the skeletal muscle of old mice. *Journal of Anatomy*, *228*(5), 771–783. https://doi.org/10.1111/joa.12429

Coffey, V. G., & Hawley, J. A. (2007). The molecular bases of training adaptation. *Sports Medicine*, *37*(9), 737–763. https://doi.org/10.2165/00007256-200737090-00001

Dahl, K. N., Ribeiro, A. J. S., & Lammerding, J. (2008). Nuclear shape, mechanics, and mechanotransduction. *Circulation Research*, *102*(11), 1307–1318. https://doi.org/10.1161/CIRCRESAHA.108.173989

Earle, A. J., Kirby, T. J., Fedorchak, G. R., Isermann, P., Patel, J., Iruvanti, S., Bonne, G., Wallrath, L. L., & Lammerding, J. (2019). Mutant lamins cause nuclear envelope rupture and DNA damage in skeletal muscle cells. *Nature Materials*, *19*, 1–10. https://doi.org/10.1038/s41563-019-0563-5

Frontera, W. R., & Ochala, J. (2015). Skeletal muscle: A brief review of structure and function. *Behavior Genetics*, *45*(2), 183–195. https://doi.org/10.1007/s00223-014-9915-y

Goh, Q., Song, T., Petrany, M. J., Cramer, A. A., Sun, C., Sadayappan, S., Lee, S. J., Millay, D. P. (2019). Myonuclear accretion is a determinant of exercise-induced remodeling in skeletal muscle. *eLife*, *8*, e44876. https://doi.org/10.7554/eLife.44876

Hall, Z. W., & Ralston, E. (1989). Nuclear domains in muscle cells. *Cell*, *59*(5), 771–772. https://doi.org/10.1016/0092-8674(89)90597-7

Irrcher, I., Adhihetty, P. J., Joseph, A. M., Ljubicic, V., & Hood, D. A. (2003). Regulation of mitochondrial biogenesis in muscle by endurance exercise. *Sports Medicine*, *33*(11), 783–793. https://doi.org/10.2165/00007256-200333110-00001

Kurosaka, M., Naito, H., Ogura, Y., Machida, S., & Katamoto, S. (2012). Satellite cell pool enhancement in rat plantaris muscle by endurance training depends on intensity rather than duration. *Acta Physiologica*, *205*(1), 159–166. https://doi.org/10.1111/j.1748-1716.2011.02381.x

Lammerding, J., Hsiao, J., Schulze, P. C., Kozlov, S., Stewart, C. L., & Lee, R. T. (2005). Abnormal nuclear shape and impaired mechanotransduction in emerin-deficient cells. *Journal of Cell Biology*, *170*(5), 781–791. https://doi.org/10.1083/jcb.200502148

Levy, Y., Ross, J. A., Niglas, M., Snetkov, V. A., Lynham, S., Liao, C.-Y., Puckelwartz, M. J., Hsu, Y.-M., McNally, E. M., Alsheimer, M., Harridge, S. D. R., Young, S. G., Fong, L. G., Español, Y., Lopez-Otin, C., Kennedy, B. K., Lowe, D. A., & Ochala, J. (2018). Prelamin A causes aberrant myonuclear arrangement and results in muscle fiber weakness. *JCI Insight*, *3*(19), 1–18. https://doi.org/10.1172/jci.insight.120920

Lieber, R. L. (2002). Skeletal muscle structure, function, and plasticity. In: Julet, T. (Ed.), *Skeletal muscle, structure, function, and plasticity*. Lippincott Williams & Wilkins.

Lin, J., Wu, H., Tarr, P. T., Zhang, C. Y., Wu, Z., Boss, O., Michael, L. F., Puigserver, P., Isotani, E., Olson, E. N., Lowell, B. B., Bassel-Duby, R., & Spiegelman, B. M. (2002). Transcriptional co-activator PGC-1α drives the formation of slow-twitch muscle fibres. *Nature*, *418*(6899), 797–801. https://doi.org/10.1038/nature00904

Miniou, P., Tiziano, D., Frugier, T., Roblot, N., Le Meur, M., & Melki, J. (1999). Gene targeting restricted to mouse striated muscle lineage. *Nucleic Acids Research*, *27*(19), 27. https://doi.org/10.1093/nar/27.19.e27

Murach, K. A., Mobley, C. B., Zdunek, C. J., Frick, K. K., Jones, S. R., McCarthy, J. J., Peterson, C. A., & Dungan, C. M. (2020). Muscle memory: Myonuclear accretion, maintenance, morphology, and miRNA levels with training and detraining in adult mice. *Journal of Cachexia, Sarcopenia and Muscle*, *11*, 1705–1722. https://doi.org/10.1002/jcsm.12617

Neubauer, O., Sabapathy, S., Ashton, K. J., Desbrow, B., Peake, J. M., Lazarus, R., Wessner, B., Cameron-Smith, D., Wagner, K. H., Haseler, L. J., & Bulmer, A. C. (2014). Time course-dependent changes in the transcriptome of human skeletal muscle during recovery from endurance exercise: From inflammation to adaptive remodeling. *Journal of Applied Physiology*, *116*(3), 274–287. https://doi.org/10.1152/japplphysiol.00909.2013

Pavlath, G. K., Rich, K., Webster, S. G., & Blau, H. M. (1989). Localization of muscle gene products in nuclear domains. *Nature*, *337*(6207), 570–573. https://doi.org/10.1038/337570a0

Pérez-Schindler, J., Summermatter, S., Santos, G., Zorzato, F., & Handschin, C. (2013). The transcriptional coactivator PGC-1α is dispensable for chronic overload-induced skeletal muscle hypertrophy and metabolic remodeling. *Proceedings of the National Academy of Sciences of the United States of America*, *110*(50), 20314–20319. https://doi.org/10.1073/pnas.1312039110

Petrella, J. K., Kim, J.-S, Mayhew, D. L., Cross, J. M., & Bamman, M. M. (2008). Potent myofiber hypertrophy during resistance training in humans is associated with satellite cell-mediated myonuclear addition: A cluster analysis. *Journal of Applied Physiology*, *104*(6), 1736–1742. https://doi.org/10.1152/japplphysiol.01215.2007

Pilegaard, H., Saltin, B., & Neufer, D. P. (2003). Exercise induces transient transcriptional activation of the PGC-1α gene in human skeletal muscle. *Journal of Physiology*, *546*(3), 851–858. https://doi.org/10.1113/jphysiol.2002.034850

Relaix, F., & Zammit, P. S. (2012). Satellite cells are essential for skeletal muscle regeneration: The cell on the edge returns centre stage. *Development*, *139*(16), 2845–2856. https://doi.org/10.1242/dev.069088

Ross, J. A., Pearson, A., Levy, Y., Cardel, B., Handschin, C., & Ochala, J. (2017). Exploring the role of PGC-1α in defining nuclear organisation in skeletal muscle fibres. *Journal of Cellular Physiology*, *232*(6), 1270–1274. https://doi.org/10.1002/jcp.25678

Sassoon, D. A., Garner, I., & Buckingham, M. (1988). Transcripts of α-cardiac and α-skeletal actins are early markers for myogenesis in the mouse embryo. *Development*, *104*(1), 155–164.

Scarpulla, R. C. (2011). Metabolic control of mitochondrial biogenesis through the PGC-1 family regulatory network. *Biochimica et Biophysica Acta–Molecular Cell Research*, *1813*(7), 1269–1278. https://doi.org/10.1016/j.bbamcr.2010.09.019

Schreiber, S. N., Emter, R., Hock, M. B., Knutti, D., Cardenas, J., Podvinec, M., Oakeley, E. J., & Kralli, A. (2004). The estrogen-related receptor α (ERRα) functions in PPARγ coactivator 1α (PGC-1α)-induced mitochondrial biogenesis. *Proceedings of the National Academy of Sciences of the United States of America*, *101*(17), 6472–6477. https://doi.org/10.1073/pnas.0308686101

Schreiber, S. N., Knutti, D., Brogli, K., Uhlmann, T., & Kralli, A. (2003). The transcriptional coactivator PGC-1 regulates the expression and activity of the orphan nuclear receptor estrogen-related receptor α (ERRα). *Journal of Biological Chemistry*, *278*(11), 9013–9018. https://doi.org/10.1074/jbc.M212923200

Smith, H. K., & Merry, T. L. (2012). Voluntary resistance wheel exercise during post-natal growth in rats enhances skeletal muscle satellite cell and myonuclear content at adulthood. *Acta Physiologica*, *204*(3), 393–402. https://doi.org/10.1111/j.1748-1716.2011.02350.x

Stroud, M. J., Feng, W., Zhang, J., Veevers, J., Fang, X., Gerace, L., & Chen, J. (2017). Nesprin 1α2 is essential for mouse postnatal viability and nuclear positioning in skeletal muscle. *Journal of Cell Biology*, *216*(7), 1915–1924. http://doi.org/10.1083/jcb.201612128

Stroud, M. J., Fang, X., Zhang, J., Guimarães-Camboa, N., Veevers, J., Dalton, N. D., Gu, Y., Bradford, W. H., Peterson, K. L., Evans, S. M., Gerace, L., & Chen, J. (2018). Luma is not essential for murine cardiac development and function. *Cardiovascular Research*, *114*(3), 378–388. http://doi.org/10.1093/cvr/cvx205

Uldry, M., Yang, W., St-Pierre, J., Lin, J., Seale, P., & Spiegelman, B. M. (2006). Complementary action of the PGC-1 coactivators in mitochondrial biogenesis and brown fat differentiation. *Cell Metabolism*, *4*(1), 97–41. https://doi.org/10.1016/j.cmet.2006.06.005

Wu, Z., Puigserver, P., Andersson, U., Zhang, C., Adelmant, G., Mootha, V., Troy, A., Cinti, S., Lowell, B., Scarpulla, R. C., & Spiegelman, B. M. (1999). Mechanisms controlling mitochondrial biogenesis and respiration through the thermogenic coactivator PGC-1. *Cell*, *98*(1), 115–124. https://doi.org/10.1016/S0092-8674(00)80611-X

SUPPORTING INFORMATION

Additional Supporting Information may be found online in the supporting information tab for this article.

How to cite this article: Battey, E., Furrer, R., Ross, J., Handschin, C., Ochala, J., & Stroud, M. J. (2021). PGC-1α regulates myonuclear accretion after moderate endurance training. *Journal of Cellular Physiology*, 1–10. https://doi.org/10.1002/jcp.30539